

# Evaluation Of Various Rainfall-Runoff Models: A Case Study Of The Nakhla Catchment, North Of Morocco

Elamine Boubkir<sup>1</sup>, Rachid Bouchnan<sup>2</sup>, Mohamed Draoui<sup>3</sup>

<sup>1,2,3</sup>Biology, Environment, and Sustainable Development Laboratory, École Normale Supérieure (ENS), Abdelmalek Essaâdi University, Tétouan 93000, Morocco

Corresponding author: Elamine Boubkir; [elamine.boubkir@etu.uae.ac.ma](mailto:elamine.boubkir@etu.uae.ac.ma)

---

## ABSTRACT:

The Mediterranean climate characterized by large variation in rainfall intensity and duration, represents a major challenge for accurate hydrological prediction and simulation. Therefore, we aim by the present study to compare the accuracy of several rainfall-runoff models. We tested several configurations of models in the watershed called Nakhla, located in northern Morocco, over the period from 2004 to 2014, using inputs including the land use, soil and hourly meteorological data. The calibrated results were compared with the observed runoff data from the dam of Nakhla which represents the watershed outlet. The result analysis was made by application of performance indicators including the correlation coefficient, RMSE,  $R^2$ , Pbias, and NSE. Generally, the results of all models tested showed good performance. However, the analysis revealed that the Smith Parlange model was the most accurate model, while the SCS Curve number was classified in the second range. The Green and Ampt, along with the Initial, Deficit and Constant models showed the lower performances. The present study provides methodological framework to adopt the appropriate model in different hydrological contexts. In addition, these results could provide decision-making tools for water resource management.

## Keywords:

rainfall-runoff models; loss models; Nakhla catchment; SCS curve number; deficit and constant; initial and constant; Green and Ampt; Smith Parlange; Clark unit hydrograph; Snyder unit hydrograph;

---

## INTRODUCTION

Simulating runoff has always been a complex challenge, especially for water management, environmental planning, and flood prediction. Therefore, many runoff models have been created, whose performances vary depending on zone characteristics such as slope inclination, land use and climate conditions [1].

In term of complexity and approach, the runoff models could vary between 3 types, ranging from empirical methods to conceptual and physically-based model types. For instance, the empirical models such as the SCS (Soil Conservation Service) Curve Number model [2] is based on observations of several components of the hydrological process and their relationships. It is often simplified and requiring less data. Conceptual models, like the TOPMODEL (Topography-Based Hydrological MODEL) [3], the HBV model (Hydrological Byranes water department model) [4]..., attempting a balance between the simplicity of empirical and the complexity of physically-based models. Reaching it by presenting the general hydrological process without including details of each process interactions. Moreover, the Physically-based models are more complex by using equations simulating the water movement and storage, like MIKE-SHE [5], Green and Ampt Loss [6], and Richards equation [7]...

Several researchers have compared multiple methods to evaluate their performances across different geographical and climatic conditions. Such as [8] study where they compared the accuracy of two models, the SCS and Green-Ampt models In Senegal's Nbidia catchment. They validate the models by 28 rainfall-runoff events, using the Nash-Sutcliffe Efficiency (NSE) coefficient. Another experimental study evaluated five rainfall loss methods, including the Green and Ampt, the Smith Parlange, the Initial and Constant, the SCS Curve Number, and the Horton. [9] tested their accuracy contrasted to the observed experimental data, by employing a ranking system from 0 to 3. The score of 3 indicated that the method fully matched the observed experimental results. Furthermore, [10] compared the SCS CN and Green-Ampt Mein-Larson methods in the Goodwin Creek Watershed, both models were primarily evaluated by the NSE and  $R^2$ .

Application of similar studies in different environmental conditions could enhance the understanding of runoff-models. Therefore, our work is in line with this approach, by evaluating five loss models (Deficit Constant, Initial Constant, Green and Ampt, SCS CN and Smith Parlange), combined with Clark unit hydrograph (UH) and Snyder UH transforming models.

Furthermore, to assess the accuracy of each configuration, we used five performance keys: the correlation coefficient, RMSE,  $R^2$ , Pbias and NSE. The latter keys are used to assess the relationship between predicted and observed runoff, the magnitude of prediction errors, and the overall efficiency of the model in simulating runoff behavior.

This study was performed on the Nakhla dam watershed, in NW Morocco, which was selected based on several key-considerations, mainly, the accessibility and availability of the required data.

The present study offers a methodology to assess the performances of several runoff models, by comparing their accuracy, which could be applied in similar catchments. Moreover, this work provides decision-making tool to select and use of the adequate runoff-model for water resources management purposes.

## MATERIALS AND METHODS

### Study area

The present study area is located between Tetouan and Chefchaouen Cities, in the north-western part of Morocco (Fig. 1b). It occupies an area of 110. 20 square kilometers ( $Km^2$ ), drained on 16,75 kilometers (km) by the river of Hajera and its tributaries.

This river is characterized by low flow over the year, with a slight increasing in runoff values during the wet season. This flow pattern is caused by the presence of extensive vegetation cover along the river, combined with a moderated slope along the Hajera River.

The slope of the study area varies between 617.17% in the eastern zones and 0.003% in the northern part, and the medium slope of the watershed is reaching 36.51%. The elevation gradient also varies in the Nakhla watershed, with the highest point reaching 1801 meters (m) in the southeast and the lowest at 164 meters in the northwest (Fig. 1a).

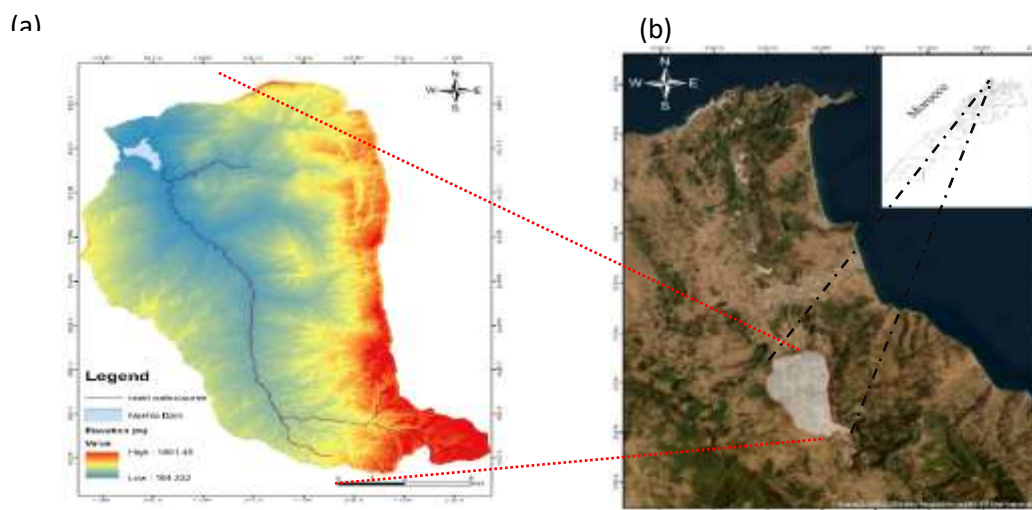


Figure 1: (a) Digital elevation model and the hydrographic network; (b) Study area location

At the outlet of our watershed, the Nakhla Dam is an embankment rock-fill structure, built in 1961 to supply water and irrigation for the city of Tetouan and surrounding areas. At the Normal Operating Water Level of 190.65 meters, this dam was initially built with a storage capacity of 9 million cubic meters ( $m^3$ ). However, according to the siltation monitoring, the dam capacity has been reduced to 4.2 million cubic meters, representing a loss of 53.34% of the dam's storage capacity [11].

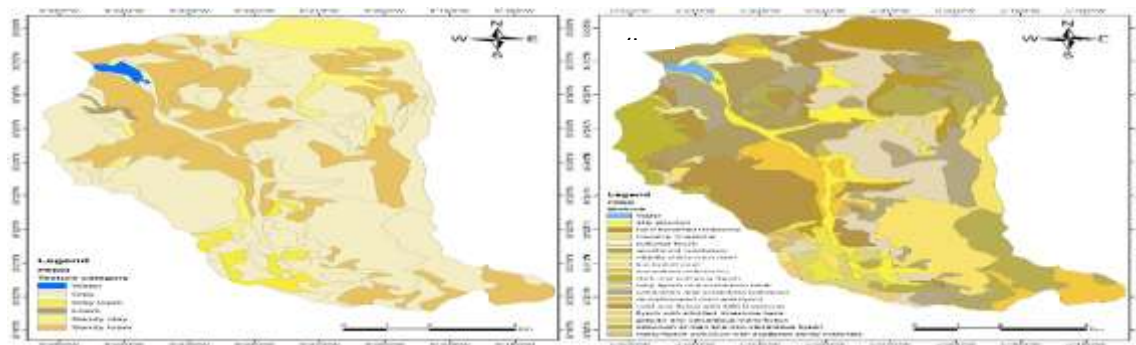


Figure 2: (a) Soil texture classification of the Nakhla watershed; (b) bedrock composition of the study area

Based on the study made by [12], the watershed is dominantly occupied by clayey soils, accounting for 61.43%, suggesting low permeability and high-water retention capacity. In contrast, sandy-loam soils covering approximately 27.71%, increase infiltration and water movement through the soil profile. These later soils are more vulnerable to water erosion. The other minor soil types are the clay loam and loam areas, representing less than 10% of the area (Fig. 2).

The land use of Nakhla catchment is characterized by the dominance of two classes, including the forest and the bare ground occupying respectively, 42.4% and 41.58%, indicating an unmodified natural landscape. The other classes, such as the developed zones and irrigated crops, are limited, comprising 1.72% of the total area (Fig. 3).

In addition, the Nakhla watershed is characterized by a sub-humid Mediterranean climate, occurring in hot and dry summers from May to September and wet winters from October to March. The highest recorded rainfall was in December 1996, with 525.5 millimeters (mm) recorded in one month. The annual rainfall average is 706.3 millimeters.



Figure 3: Land-use map of the Nakhla watershed

#### Data acquisition and pre-processing

Soil data for the study area were generated based on a soil study carried out in the Nakhla watershed with the support of the Ministry of Environment and the United States Agency for International Development (USAID) [12].

Soil hydraulic parameters data, such as total porosity, residual saturation, effective porosity, bubbling pressure, pore size distribution index, and saturated hydraulic conductivity, were derived based on several soil texture data references, including studies by [13], [14], and [15].

The land use data of the Nakhla watershed was digitalized based on 1/25000 topographic maps:

- AL HAMRA NI-30-XIX-2-c-2
- TAYENZA NI-30-XIX-2-c-1
- ZINAT NI-30-XIX-2-c-3
- OUED EL KHEMIS NI-30-XIX-2-c-4

These topographic maps were updated from aerial shots taken in March 2015, and partially completed in the field in October 2017 by the National Agency for Land Conservation, Cadaster and Cartography (ANCFCC).

In addition, the rainfall data of the study zone was based on the combination of two types of data. The first type was based on a measured daily data provided by the Loukkos River Basin Agency (ABHL), collected from 3 Rain gauge stations located in or near to the Nakhla watershed. The second type was founded based on an hourly rainfall simulated by NASA project called Integrated Multi-satellitE Retrievals for GPM (IMERG). The two types of data sources were crucial, as the objective was to extract the hourly patterns from the NASA data and apply them to the measured data. This approach allowed us to obtain the hourly measured data for the study area over a 10-year period. Afterwards, we have filtrated the outcome by eliminating the dry days and those recording less than 0.1 mm. The results of this filtration provide an initial identification of the wet events. Furthermore, in order to identify the wet events, we separated the events with minimum dryness intervals of four hours. These procedures are essential, since the current study is focused exclusively in the wet event to simulate the long-term runoff.

Furthermore, the daily evaporation data were similar to the rainfall data. It was based on a data provided and measured by the ABHL, essentially by using their gauging stations.

cartographic sources obtained from the ANCFCC. The contours were manually digitized and subsequently interpolated. The validation procedure was based on control points, which we compared between the interpolated digital elevation model and the original topographical cartographic reference. This validation process revealed an average relative error of 0.026%.

Moreover, the concentration time ( $T_c$ ), which is an essential key of the transforming methods, was calculated for the watershed sub-basins based on the mean of two widely recognized formulas: Giandotti, and the Témez formula [16,17].

#### **Hydrological Model Configuration**

Given the canopy occupies 57,15% of the total Nakhla watershed area (Fig.4), it's critical to simulate it in order to understand and model the hydrological system. We chose a model called the simple canopy model to evaluate the canopy interception based on the land cover map. The key parameters of this model are the canopy storage and the crop coefficients, which were based on several similar studies [19], combined with [20], [21], [22], and [23] studies.

Moreover, the steepness of the slope in the catchment, which increases the flow velocity and reduces the water retention capacity, justifies the exclusion of water retention simulation. In this fact, this factor is considered negligible in the Nakhla watershed.



Figure 4: Example of the canopy of the Nakhla Watershed



Furthermore, a base flow rate was detected in the data of the two existing gauging stations, the Nakhla and Jbel Timerzouk stations. These insights were confirmed by the following satellite picture in Fig. 5, acquired on January 1, 2005 by the MODIS (Moderated Resolution Imaging Spectroradiometer) sensor onboard the Terra satellite [24]. Proving as an example, a clear sky where no clouds/rainfall is occurring. Parallel, the data from gauging stations confirms the presence of a permanent flow at this date, attesting the existence of a considerable base flow.



Figure 5: satellite image acquired by Terra, MODIS on January 1, 2005. [24]

For the goal of a base flow separation, we adopted a recursive digital filter proposed by [25], especially for its suitability for an automated processing for long-term data, and its worldwide application, as it applied for example in a more than 3300 watersheds, in a study conducted by [26].

The Eckhardt filter is based on two key parameters, the *BFI max* representing the maximum value of the base flow index. The *BFI max* values were suggested between 0.25 and 0.8 by [25], depending on the perennality of the stream and the geology of the zone. While the  $\alpha$ , representing a digital-filter constant determined by recession analysis.

In our study, the *BFI max* is fixed at 0.8, in line with geological characteristics dominated by the karst formations [27] and a perennial stream by being waterless during less than 10% of the year. The parameter  $\alpha$  was estimated 0.8966, from a recession analysis over a dry period [28].

### Hydrological Loss Methods

The loss methods in hydrology define models accounting for rainfall amounts that are not contributing in a direct runoff, which represents a loss in the hydrological system. In the present study, we used the following loss methods:

#### SCS Curve Number Loss (SCS CNL)

The SCS Curve Number (SCS) was developed by the Natural Resources Conservation Service (NRCS) for directly simulating the runoff hydrological process [15]. Moreover, an adapted version of the SCS model was introduced in the HEC-HMS (Hydrologic Engineering Center - Hydrologic Modeling System) application to simulate the hydrological loss separately [29].

The fundamental of the SCS-CN method is illustrated as Eq. (1) [29]:

$$Q = \frac{(P - Ia)^2}{(P - Ia) + S} \quad (1)$$

Where: Q: depth of runoff (mm), P: depth of rainfall (mm), Ia: initial abstraction (mm), and S: maximum soil retention (mm).

The maximum soil water storage is calculated using Eq. (2) [29]:

$$S = \frac{1000}{CN} - 10 \quad (2)$$

Where CN is a dimensionless value ranging from 30 to 100, representing the potential runoff, with higher values representing high runoff potential.

The SCS curve number loss method needs the following key parameters:

- The curve number was estimated by using standardized tables, suggesting CN value based on the land use and the soil hydrological groups [29]. The latter were determined based on infiltration rates and other characteristics [30].

- Initial Abstraction Ratio: representing the ratio of the initial loss which could be adapted for calibration purposes.

This parameter can be quantified using a variety of formulations, including these most well-known three formulas (Eq. (3), (4), and (5)):

- $Ia = 0,2 \times S$  [31] (3)

- $Ia = -0,1 \times \ln(S) + 0,3518$  [32] (4)

- $Ia = 0,05 \times S$  [33] (5)

- Potential Retention Scale Factor: It represents the potential for water retention, its default number in the HEC HMS application is 1. This parameter could be adapted for calibration purposes.

#### *The Deficit and Constant Loss (DCL)*

The Deficit and Constant Loss (DCL) model is a hydrological conceptual model, simulating hydrological rainfall-runoff processes. It has been widely applied in semi-arid regions ([34];[35] ...). In this model the soil is considered as a reservoir with a fixed storage capacity, resulting the runoff and percolation if the capacity is full [36].

The DCL concept divides the process into three major steps, as illustrated in Fig. 6:

1. The initial deficit represents an initial phase when the rain is accumulated in the soil without producing runoff or percolation, as the soil has not reached its maximum capacity.
2. Transition is defining the phase when the soil remains unsaturated and the continued rainfall increases the soil's moisture.
3. The saturation phase represents the final step, as the rainfall exceeds the soil storage capacity generating surface runoff and percolation.

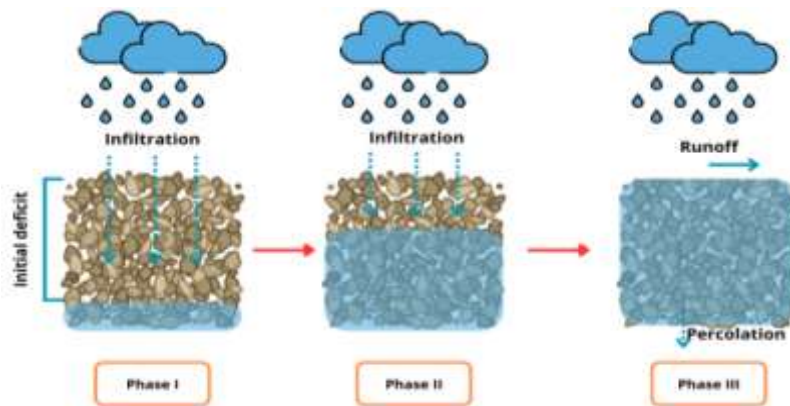


*Figure 6: Conceptual Representation of the Initial/Deficit and Constant Loss Method: Soil Moisture Dynamics and Runoff Generation Phases*

The key parameters of the model are the initial deficit, the maximum deficit, the constant rate, and the impervious zone. These parameters were used essentially for simulating the soil infiltration of the watershed.

The initial deficit represents the initial condition of the soil moisture. The maximum deficit is defined as the maximum storage capacity of the soil (m) and the constant rate defined the vertical hydraulic conductivity of the soil (meter/hour (m/hr)).

Those parameters were estimated based on soil characteristics of the study area, according to the manual of [37].

#### *Initial and constant loss (ICL)*

The Initial and Constant Loss Model (ICL) is also a conceptual loss method used for simulating the rainfall-runoff process. The ICL concept considers that certain rainfall amount is initially lost due to

interception, depression storage, and initial infiltration before the generating of the runoff [36]. The ICL considers an initial constant loss firstly impacts the hydrological system [15].

The ICL key parameters are: the initial loss and the constant loss rate. The first one represents the initial hydrological loss that should be satisfied before the runoff begins [36]. However, the second key parameter represents the soil infiltration capacity after the satisfaction of the initial losses [15].

In our study, we estimated those parameters based on guidelines and formulas provided by [36], in which we used soil characteristics, land use data and taking into account the previous moisture condition.

#### Green and Ampt Loss (GAL) [6]

The Green and Ampt loss method represents a physical based model simulating the infiltration and runoff processes during rainy events.

This model takes into account the infiltration of precipitation through a wetting front. During the rainy event, the wetting front continuous to downward into the soil, keeping a clear moisture difference between the saturated soil above and the drier soil below (Fig. 7).

The main equation of the Green-Ampt method is illustrate as Eq. (6) [36]:

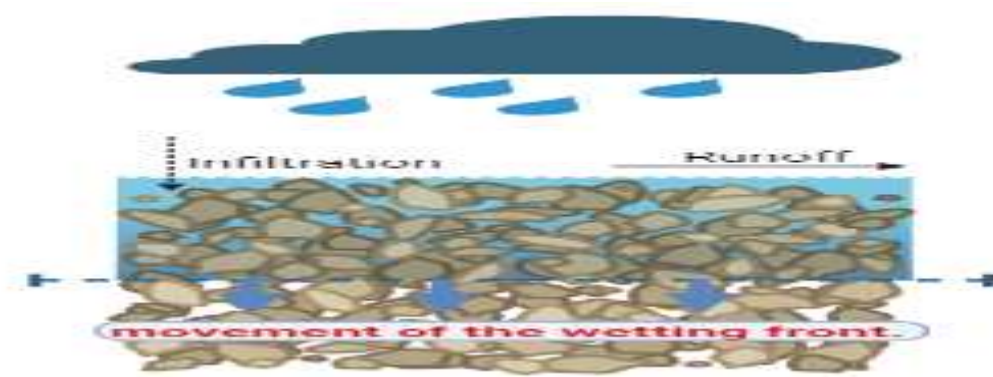


Figure 7: Conceptual representation of the Green and Ampt loss method: wetting front dynamics

$$f_t = K \left( \frac{1 + (S_f(\theta_s - \theta_i))}{F_t} \right) \quad (6)$$

Where  $f_t$  represents the loss during period (mm/hr),  $S_f$  represents the suction head at the wetting front (mm),  $\theta_s$  represents the saturated soil moisture content (fraction),  $\theta_i$  represents the initial soil moisture content (fraction),  $K$  represents the saturated hydraulic conductivity (mm/hr) and  $F_t$  represents the cumulative loss at the time  $t$  (mm). The initial soil moisture representing the initial soil water amount before the beginning of infiltration.

#### Smith Parlange Loss (SPL) [38]

This model is a physical based method used to estimate the water loss due to infiltration, representing a developed version of the Green-Ampt model. This model integrates the principles of the two-term infiltration equation proposed by [39]. The basic form of the infiltration rate (mm/hr) can be expressed as follows Eq. (7):

$$f(t) = K_{sat} \times \frac{\Psi(\theta_s - \theta_i)}{(F(t)) + 1} \quad (7)$$

Where  $K_{sat}$  represents the saturated hydraulic conductivity (mm/hr),  $\Psi$  the wetting front suction (mm),  $\theta_s$  the soil porosity (fraction),  $\theta_i$  the initial soil moisture content (fraction), and  $F(t)$  the cumulative infiltration at time  $t$  (mm).

Compared to previous used models, this model takes into account new parameters such as the residual content representing the water content retained under high suction, the pore size distribution index characterizing pore size distribution and the bubbling pressure defining the suction needed to initiate the largest pore drainage. Similar to the previous models, the entire set of key parameters was estimated based on soil characteristics.

#### Hydrological Transform Methods

In hydrology, the transform models are used to convert the excess rainfall into a direct runoff. In the present study, we used two transform models, which vary in levels of complexity and applicability in various environmental conditions:

#### *Clark Unit Hydrograph (CUH)*

This method was developed by Clark C.O. in 1945, in which he integrates the time-area histogram with a linear reservoir model [40]. It simulates the conversion of the rainfall excess, and the reduction in flow due to storage effects.

Based on Clark's equation [40], the linear reservoir model is represented as Eq. (8):

$$Q(t) = \frac{1}{Tr} \int_0^t \left( Q_{in}(\tau) e^{-\frac{(t-\tau)}{Tr}} d\tau \right) \quad (8)$$

Where  $Q(t)$ : outflow hydrograph (meter cubic per Second ( $m^3/s$ )),  $Q_{in}(\tau)$ : inflow hydrograph ( $m^3/s$ ), and  $Tr$ : storage coefficient (hr).

In order to apply the CUH, we needed the following key parameters:

- Time of Concentration ( $T_c$ ): time that takes the furthest drop of rainfall to arrive at the outlet. As we explained earlier, we did estimate the  $T_c$  using the average of two well recognized formulas: Giandotti [16] and Témez formula [17]
- Storage Coefficient ( $R$ ): storage and delay of the water flow, we estimated it by using Sabol's Equation (Eq. (9)) [41]:

$$R = \frac{T_c \times A}{1.46 - 0.0867 \times L^2} \quad (9)$$

Where  $L$ : longest water path length (m) and  $A$ : drainage area (meter square ( $m^2$ )).

#### *Snyder Unit Hydrograph (The Fort Worth District Method) (SUH-FWDM)*

The main method was developed by Snyder in 1938. It is an empirical approach based on UH shape suitable for a catchment [42]. This method has been widely applied in the semi-arid region [43].

In this paper, Franklin provides the SUH-SM key Eq. (10) and (11). The two equations are focused on calculating the watershed peak time and discharge using several parameters:

$$Tp = Ct (L \times Lc)^{0.3} \quad (10)$$

$$Qp = \frac{640 \times Cp \times A}{Tp} \quad (11)$$

Where the  $Tp$ : peak time (hr),  $L$ : length of the mainstream (m),  $Lc$ : length to the basin centroid (m),  $Ct$  and  $Cp$ : empirical coefficients (fraction),  $Qp$ : peak discharge ( $m^3/s$ ).

The SUH-SM key parameters required in the HEC-HMS are:

- The lag time ( $Tp$ ): time delay between the centroid of the rainfall mass to the peak of the UH. It was calculated using the formula proposed by [42]:  $Tp = 5.5 T_c$  with  $T_c$  is concentration time
- Peak coefficients ( $Cp$ ), varying between 0.4 and 0.94, was derived from regional data, and adjusted to improve accuracy.

The SUH-FWDM is a regional adaptation of the Snyder standard method, developed by the U.S. Army Corps of Engineers, Ft. Worth District to be adapted in the Dallas-Ft Worth, Austin, and San Antonio regions and other similar areas [44,45]. The adaptation was made by introducing new peak and lag coefficients and an internal regional equation [46].

This model requires six key parameters: the total length of the main watercourse, the centroidal length, the urbanization percentage, the slope of the main watercourse, the sand percentage and the peaking coefficient. These parameters were estimated based on land use, soil, hydrological, and slope...

#### **Statistical Performance Analysis**

The model performance was evaluated using statistical metrics to assess both the magnitude and pattern of the simulated results compared to observed data. These metrics include the correlation coefficient ( $r$ ), Root Mean Square Error (RMSE), Coefficient of Determination ( $R^2$ ), and systematic bias.

#### *Percent Bias (PBIAS)*

This analysis indicates the model systematic under- or over-prediction behavior expressed as a percentage. The Pbias formula is indicated as Eq. (12) [47]:

$$PBIAS = \left( \frac{\sum_{i=1}^{i=n} (O_i - S_i)}{\sum_{i=1}^{i=n} O_i} \right) \times 100 \quad (12)$$



Where  $O_i$ : observed value for the  $i^{\text{th}}$  observation,  $S_i$  simulated value for the  $i^{\text{th}}$  observation, and  $n$  as the number of observations

The positive values of the PBIAS represent overestimation bias, and the negative values represent underestimation bias. The accurate model bias should have the 0 value of the Pbias.

#### Nash-Sutcliffe Efficiency (NSE)

The Nash-Sutcliffe Efficiency (NSE) was introduced by [48] in their paper on river flow forecasting. The NSE is a statistic tool that determines the relative magnitude of the residual variance compared to the measured data variance. The NSE formula is written as Eq. (13):

$$NSE = 1 - \frac{\sum_{i=1}^n (O_i - \bar{O})^2}{\sum_{i=1}^n (O_i - S_i)^2} \quad (13)$$

Where  $O_i$ : observed value for the  $i^{\text{th}}$  observation,  $S_i$ : simulated value for the  $i^{\text{th}}$  observation,  $\bar{O}$ : mean of observed values,  $n$ : number of observations.

The NSE could range from negative infinity to 1, where the 1 represents the best model accuracy.

## RESULTS

As illustrated in Figure 8, we considered 18 sub-basins, delimited in QGIS (Quantum Geographic Information System) 3.38.0 and HEC-HMS 4.11 applications.

The Curve number parameter was determined by using soil texture and land use data, resulting in a raster file illustrated in Figure 9. As for the initial water content, the initial and the maximum deficit parameters, were derived from the soil and moisture data. The resulting raster shape parameters are illustrated in Figure 10, 11 and 12.

In the purpose to facilitate the citation, a reference code was created for each model combination, as illustrated in the flow chart presented in Figure 13. We calibrated and evaluated every combination performance based on the actual inflow values ( $\text{m}^3/\text{s}$ ) using key performance indicators, including the correlation coefficient, RMSE,  $R^2$ , Pbias, and NSE, presented in Table 1.

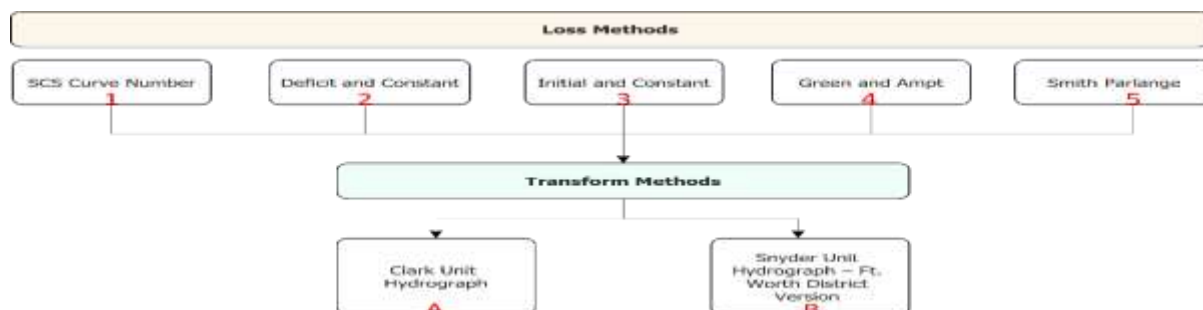


Figure 8: Flow chart of method combinations

By analyzing the used statistical performances, the method combination results can be classified from high to the low performances as follows:

- The Smith-Parlange
- The SCS Curve Number
- The Deficit and Constant
- The Green and Ampt
- The Initial and Constant

The simulation results present that the series 5 (Smith Parlange) shows generally constant coefficients for all the transform methods. As they reach 0.87, 0.75 and 0.99 respectively for correlation,  $R^2$  and NSE.

The SCS curve number series shows a variable performance between the combinations. The 1-B combination (the SCS Curve Number combined with the Ft Worth District) presents coefficients calculated as: 0.78, 74.97, 0.61, -83.39 and 0.30, respectively, for the correlation, RMSE,  $R^2$ , Pbias and NSE. The 1-A combination (the SCS Curve Number combined with the Clark UH) present correlation coefficient equals to 0.76 and 0.57 for the  $R^2$ .

The deficit and constant series presents similar results for the two combinations, with 0.77, 91.38, 0.59, -101.63 and -0.03, respectively, for the correlation coefficient, RMSE,  $R^2$ , Pbias and NSE.

The fourth series (Green and Ampt) shows a constant result across the statistical performance analysis: the correlation coefficient (0.77), RMSE (99.29),  $R^2$  (0.59), Pbias (-110.43), and the NSE (-0.22). Finally, and close to the results of the Green and Ampt series, the initial and constant results exhibit the correlation coefficient (0.77), RMSE (99.31),  $R^2$  (0.59), Pbias (-110.43), and the NSE (-0.22). similar across all the combinations.

## DISCUSSION

The Smith-Parlange loss model results demonstrated as the most effective performance compared to the other models. Indeed, with the strongest correlation coefficient (0.87). Likewise, the low values of RMSE ( $\sim 6.58$ ), Pbias near to zero (-7.32), and an NSE near to one (0.99), indicate high performance. Figure 14 below illustrates the calibrated linear trend analysis.

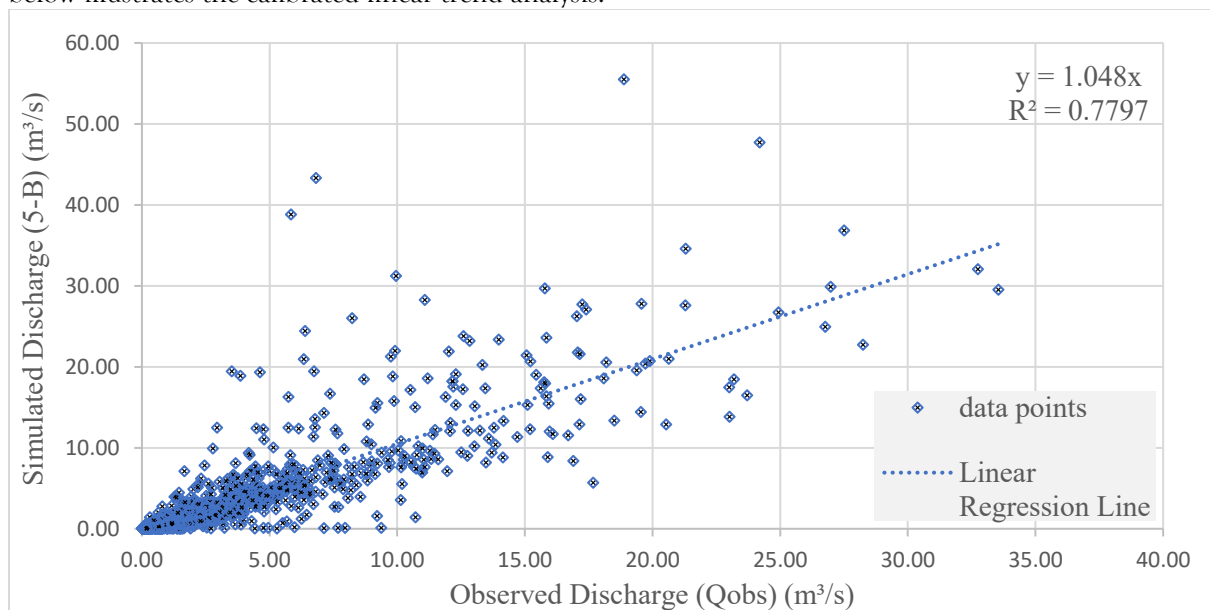


Figure 9: The linear regression line of the Smith Parlange combined with the Snyder unit hydrograph, the Worth district version

This performance agrees with several studies in the literature. A study conducted by [49], comparing fourteen infiltration methods, showed that the Smith-Parlange was among of the top performing models, by using the NSE criterion. Furthermore, [50], by comparing seven loss methods, they found that the methods of accounting infiltration capacity like Smith Parlange model, are generally better at the hill slope zones during intermittent rain.

The higher performance of the Smith Parlange can be explained by their formula based on the physical concept of providing a well-detailed description of the infiltration processes. Furthermore, the model integrates multiple physical parameters, directly measured, such as the pore size distribution index, the bubbling pressure.

As well, the A and B combinations of SCS CN model has shown a good performance, which can be related to the semi-empirical formulation of the SCS based on the main parameter "CN". The latter is an empirical approximation derived from correlation between physical properties and hydrological data from different contexts. It is calculated on the basis of multiple watershed characteristics, such as soil types, land use and the antecedent runoff condition.

The other methods; Green and Ampt, the Initial and Constant, and the Deficit and Constant methods, although achieving a good performance (correlation coefficient around 0.77), they showed a lower performance compared to the upper models. These results could be explained by high degree of simplification reducing the number of parameters describing the infiltration. Indeed, the consideration of a constant infiltration rate or uniform initial deficiency, represent globally divergence compared to the complexity of natural context.

The following figure 15 illustrates a results comparison of two contrasting combinations; 5-B as one of the higher achieving performances and 3-B as an example of the three less performance methods. The

simulated/calibrated inflow (orange line) and observed inflows (blue line) presenting the data for over a 10-year period, highlighting higher accuracy of reproducing the flow peaks for the 5-B, and an underestimation of the peaks for the 3-B.

Overall, the present approach evaluates different hydrological model performances, revealing a higher accuracy of the Smith Parlange and SCS CN methods. However, these results remain limited to the context of the watershed studied, and need to be extended to other hydrogeological environments, in order to verify their accuracy.

## CONCLUSION

The present study provides a comparative approach of different runoff models. They are conceptualized by the combination of various loss and transform models. The performances were compared on the basis of different statistical indexes.

The application was performed in the Nakhla watershed, characterized by high steepes and a large green area. In the outlet, the runoff and the reservoir volume are daily gaged in the Nakhla dam. Those observations data were used in calibration and validation process.

The results are generally presenting a good accuracy. In this context, the Smith Parlange method revealed to be the higher accurate model compared to the other methods with strong correlation (0.87). In the second range, the SCS curve number presents a good performance, specially, with the Snyder (Fort Worth District) transform model (0.78). The Green and Ampt, the Initial, the Deficit and Constant models showed a lower performance compared to other applied methods.

The high performance of Smith Parlange model could be explained by its rigorous physical concept, based on multiple directly measured parameters, allowing more accuracy of the results. As well, the good performance of the SCS CN model could be due to its semi-empirical concept based on the CN parameter resulting from different statistical studies used on different watersheds data. The results of the other models presenting lower performances are generally explained by their exaggerated simplification which could alter the results compared to the reality.

## REFERENCES

- [1] Devia, G. K., Ganasri, B. P., and Dwarakish, G. S., 2015, "A Review on Hydrological Models," *Aquat. Procedia*, 4, pp. 1001–1007. <https://doi.org/10.1016/j.aqpro.2015.02.126>.
- [2] Mishra, S. K., and Singh, V. P., 2013, *Soil Conservation Service Curve Number (SCS-CN) Methodology*, Springer Science & Business Media.
- [3] Kirkby M., 1975, "Hydrograph Modeling Strategies," *Process Phys. Hum. Geogr.*, pp. 69–90.
- [4] Bergström, S., 1976, Development and Application of a Conceptual Runoff Model for Scandinavian Catchments.
- [5] Abbott, M. B., Bathurst, J. C., Cunge, J. A., O'Connell, P. E., and Rasmussen, J., 1986, "An Introduction to the European Hydrological System – Systeme Hydrologique Européen, 'SHE', 2: Structure of a Physically-Based, Distributed Modelling System," *J. Hydrol.*, 87(1–2), pp. 61–77. [https://doi.org/10.1016/0022-1694\(86\)90115-0](https://doi.org/10.1016/0022-1694(86)90115-0).
- [6] WH Green, G. A., and Ampt, G. A., 1911, "Studies on Soil Physics," *J. Agric. Sci.*, 4(1), pp. 1–24. <https://doi.org/10.1017/S0021859600001441>.
- [7] Richards, L. A., 1931, "Capillary Conduction of Liquids Through Porous Mediums," *Physics*, 1(5), pp. 318–333. <https://doi.org/10.1063/1.1745010>.
- [8] Bouvier, C., Bouchenaki, L., and Trambay, Y., 2018, "Comparison of SCS and Green-Ampt Distributed Models for Flood Modelling in a Small Cultivated Catchment in Senegal," *Geosciences*, 8(4), p. 122. <https://doi.org/10.3390/geosciences8040122>.
- [9] Bezak, N., Peranić, J., Mikoš, M., and Arbanas, Ž., 2022, "Evaluation of Hydrological Rainfall Loss Methods Using Small-Scale Physical Landslide Model," *Water*, 14(17), p. 2726. <https://doi.org/10.3390/w14172726>.
- [10] K. W. King, J. G. Arnold, and R. L. Bingner, 1999, "Comparison of Green-Ampt and Curve Number Methods on Goodwin Creek Watershed Using SWAT," *Trans. ASAE*, 42(4), pp. 919–926. <https://doi.org/10.13031/2013.13272>.
- [11] ABHL, 2014, "Bathymetric Data of the Nakhla Dam (Excel File, Unpublished Data)."
- [12] Naïmi, M., and Bouabid, R., 1997, "Pedological study at 1:50,000 scale of the Nakhla watershed, (Rif Occidental) [in French]" *Proj. Pérennité Ressources. En Eau Maroc PREM Ministère L'Environnement Rabat*, 68.
- [13] Rawls, W. J., Brakensiek, D. L., and Miller, N., 1983, "Green-ampt Infiltration Parameters from Soils Data," *J. Hydraul. Eng.*, 109(1), pp. 62–70. [https://doi.org/10.1061/\(ASCE\)0733-9429\(1983\)109:1\(62\)](https://doi.org/10.1061/(ASCE)0733-9429(1983)109:1(62)).
- [14] W. J. Rawls, D. L. Brakensiek, and K. E. Saxton, 1982, "Estimation of Soil Water Properties," *Trans. ASAE*, 25(5), pp. 1316–1320. <https://doi.org/10.13031/2013.33720>.
- [15] W. Scharffenberg, 1994, *Hydrologic Modeling System HEC-HMS (USER'S MANUAL)*.
- [16] Giandotti Mario., 1933, "Forecasting floods and low flows of waterways [in Italian]"
- [17] Témez, J.R., 1978, "Hydrometeorological calculation of peak flows in small natural watersheds"

[in Spanish]" Dirección General de Carreteras, Madrid, Spain.

- [18] Aboal, J. R., Jiménez, M. S., Morales, D., and Hernández, J. M., 1999, "Rainfall Interception in Laurel Forest in the Canary Islands," *Agric. For. Meteorol.*, 97(2), pp. 73–86. [https://doi.org/10.1016/S0168-1923\(99\)00083-0](https://doi.org/10.1016/S0168-1923(99)00083-0).
- [19] David, T. S., Gash, J. H. C., Valente, F., Pereira, J. S., Ferreira, M. I., and David, J. S., 2006, "Rainfall Interception by an Isolated Evergreen Oak Tree in a Mediterranean Savannah," *Hydrol. Process.*, 20(13), pp. 2713–2726. <https://doi.org/10.1002/hyp.6062>.
- [20] Gómez, J. A., Giráldez, J. V., and Fereres, E., 2001, "Rainfall Interception by Olive Trees in Relation to Leaf Area," *Agric. Water Manag.*, 49(1), pp. 65–76. [https://doi.org/10.1016/S0378-3774\(00\)00116-5](https://doi.org/10.1016/S0378-3774(00)00116-5).
- [21] Gash, J. H. C., and Morton, A. J., 1978, "An Application of the Rutter Model to the Estimation of the Interception Loss from Thetford Forest," *J. Hydrol.*, 38(1–2), pp. 49–58. [https://doi.org/10.1016/0022-1694\(78\)90131-2](https://doi.org/10.1016/0022-1694(78)90131-2).
- [22] Loustau, D., Berbigier, P., and Granier, A., 1992, "Interception Loss, Throughfall and Stemflow in a Maritime Pine Stand. II. An Application of Gash's Analytical Model of Interception," *J. Hydrol.*, 138(3–4), pp. 469–485. [https://doi.org/10.1016/0022-1694\(92\)90131-E](https://doi.org/10.1016/0022-1694(92)90131-E).
- [23] Yerk, W., 2016, "Direct Measurements of Water Canopy Storage Capacity of Broadleaf Shrubs under Different Temperature and Wetting Regimes," 2016, pp. H31E-1430.
- [24] Jacques Desclottes, MODIS Rapid Response Team, NASA/GSFC, 2005, "NASA Earth Observatory." [Online]. Available: <https://visibleearth.nasa.gov/images/72493/morocco>. [Accessed: 30-Apr-2025].
- [25] Eckhardt, K., 2005, "How to Construct Recursive Digital Filters for Baseflow Separation," *Hydrol. Process.*, 19(2), pp. 507–515. <https://doi.org/10.1002/hyp.5675>.
- [26] Beck, H. E., van Dijk, A. I. J. M., Miralles, D. G., de Jeu, R. A. M., (Sampurno) Bruijnzeel, L. A., McVicar, T. R., and Schellekens, J., 2013, "Global Patterns in Base Flow Index and Recession Based on Streamflow Observations from 3394 Catchments," *Water Resour. Res.*, 49(12), pp. 7843–7863. <https://doi.org/10.1002/2013WR013918>.
- [27] Rampnoux, J., Angelier, J., Colletta, B., Fudral, S., Guillemin, M., and Pierre, G., 1979, "On the neotectonics evolution of northern Morocco [in French]" <https://doi.org/10.3406/geolm.1979.1114>.
- [28] Eckhardt, K., 2008, "A Comparison of Baseflow Indices, Which Were Calculated with Seven Different Baseflow Separation Methods," *J. Hydrol.*, 352(1–2), pp. 168–173. <https://doi.org/10.1016/j.jhydrol.2008.01.005>.
- [29] NRCS, 2004, "Estimation of Direct Runoff from Storm Rainfall," *Natl. Eng. Handb. Part*, 630.
- [30] USDA Natural Resources Conservation Service (NRCS), 2009, "Hydrologic Soil Groups." [Online]. Available: <https://www.hydrocad.net/neh/630contents.htm>. [Accessed: 10-Jun-2024].
- [31] Cronshey, Roger, 1986, *Urban Hydrology for Small Watersheds*, U.S. Department of Agriculture, Soil Conservation Service, Engineering Division.
- [32] Jiang, R., 2001, "Investigation of Runoff Curve Number Initial Abstraction Ratio."
- [33] Woodward, D. E., Hawkins, R. H., Jiang, R., Hjelmfelt, Jr., A. T., Van Mullem, J. A., and Quan, Q. D., 2003, "Runoff Curve Number Method: Examination of the Initial Abstraction Ratio," *World Water & Environmental Resources Congress 2003*, American Society of Civil Engineers, Philadelphia, Pennsylvania, United States, pp. 1–10. [https://doi.org/10.1061/40685\(2003\)308](https://doi.org/10.1061/40685(2003)308).
- [34] Yilma, Z. L., and Kebede, H. H., 2023, "Simulation of the Rainfall–Runoff Relationship Using an HEC-HMS Hydrological Model for Dabus Subbasin, Blue Nile Basin, Ethiopia," *H2Open J.*, 6(3), pp. 331–342. <https://doi.org/10.2166/h2oj.2023.055>.
- [35] Ndeketya, A., and Dundu, M., 2021, "Application of HEC-HMS Model for Evaluation of Rainwater Harvesting Potential in a Semi-Arid City," *Water Resour. Manag.*, 35(12), pp. 4217–4232. <https://doi.org/10.1007/s11269-021-02941-0>.
- [36] Feldman, Arlen D, 2000, "HEC-HMS Technical Reference Manual."
- [37] Department of the Army U.S. Army Corps of Engineers Washington, DC, 1994, *Flood-Runoff Analysis (ENGINEER MANUAL)*.
- [38] Smith, R. E., and Parlange, J. -Y., 1978, "A Parameter-efficient Hydrologic Infiltration Model," *Water Resour. Res.*, 14(3), pp. 533–538. <https://doi.org/10.1029/WR014i003p00533>.
- [39] Philip, J. R., 1957, "The Theory of Infiltration: I. The Infiltration Equation and its Solution," *Soil Sci.*, 83(5), p. 345.
- [40] Clark, C. O., 1945, "Storage and the Unit Hydrograph," *Trans. Am. Soc. Civ. Eng. Vol 110 No 1*. [Online]. Available: <https://ascelibrary.org/doi/abs/10.1061/TACEAT.0005800>. [Accessed: 17-Jul-2024].
- [41] Sabol, G. V., 1988, "Clark Unit Hydrograph and R-Parameter Estimation," *J. Hydraul. Eng.*, 114(1), pp. 103–111. [https://doi.org/10.1061/\(ASCE\)0733-9429\(1988\)114:1\(103\)](https://doi.org/10.1061/(ASCE)0733-9429(1988)114:1(103)).
- [42] Franklin F. Snyder, 1938, "Synthetic Unit-Graphs," *Eos Trans. Am. Geophys. Union*, 19(1), pp. 447–454. <https://doi.org/10.1029/TR019i001p00447>.
- [43] Muhammad, K. K., and Abood, P. D. A. S., 2025, "Estimating the Volume of Flash Flooding in the Wadi Qasab Basin in Khanaqin District Using the Snyder Model," *Int. J. Environ. Sci.*, pp. 19–32. <https://doi.org/10.64252/r0bh3m62>.
- [44] Nelson, T. L., 1970, "Synthetic Unit Hydrograph Relationships, Trinity River Tributaries, Fort Worth-Dallas Urban Area."
- [45] Wilbur L, M. J., 1964, "Analysis of Unit Hydrographs for Small Watersheds in Texas."
- [46] U.S. Army Corps of Engineers, 2009, "HEC-HMS Version 3.4 Release Notes."
- [47] Gupta, H. V., Sorooshian, S., and Yapo, P. O., 1999, "Status of Automatic Calibration for Hydrologic Models: Comparison with Multilevel Expert Calibration," *J. Hydrol. Eng.*, 4(2), pp. 135–143. [https://doi.org/10.1061/\(ASCE\)1084-0699\(1999\)4:2\(135\)](https://doi.org/10.1061/(ASCE)1084-0699(1999)4:2(135)).
- [48] Nash, J. E., and Sutcliffe, J. V., 1970, "River Flow Forecasting through Conceptual Models Part I – A Discussion of Principles," *J. Hydrol.*, 10(3), pp. 282–290. [https://doi.org/10.1016/0022-1694\(70\)90255-6](https://doi.org/10.1016/0022-1694(70)90255-6).